

BBA 72689

## The gramicidin A channel: theoretical energy profile computed for single occupancy by a divalent cation, $\text{Ca}^{2+}$

Catherine Etchebest, Alberte Pullman and Shoba Ranganathan

*Institut de Biologie Physico-Chimique, Laboratoire de Biochimie Théorique associé au C.N.R.S., 13, rue Pierre et Marie Curie, 75005 Paris (France)*

(Received March 1st, 1985)

Key words: Ion channel; Gramicidin A;  $\text{Ca}^{2+}$ ; Energy profile

The energy profile for the interaction of the divalent cation  $\text{Ca}^{2+}$  with the gramicidin A channel has been computed, introducing successively the different structural components of the channel, namely the polypeptide backbone, the ethanolamine tails and the amino acid side chains. The calculations have been performed in two fashions: (1) with the tail fixed in its most stable conformation, (2) with the tail allowed to optimize its conformation upon progression of the cation. The introduction of the tail and more particularly of its flexibility modifies considerably the profile. On the other hand, in both cases, the introduction of the side chains does not modify qualitatively the overall shape of the energy profile, although it brings about a general lowering of the energies. When the tail is mobile, a very deep and narrow minimum is found at 10.5 Å from the center and the central barrier is roughly 21 kcal/mol. The similarities and differences found with respect to the corresponding profiles for alkali ions,  $\text{Na}^+$  in particular, are discussed in connection with the very low permeability, if any, of gramicidin A for  $\text{Ca}^{2+}$ .

### Introduction

In the previous papers of this series [1–4], we have reported the energy profiles computed for the monovalent alkali cations,  $\text{Na}^+$ ,  $\text{K}^+$ ,  $\text{Cs}^+$  in the channel formed by gramicidin A, assumed to be in Urry's head-to-head dimeric structure [5–6] (Figs. 1a and 1b). In a first step [1], the energy profile for single and double occupancy by  $\text{Na}^+$  was computed including the entire polypeptide backbone of gramicidin A and its formyl heads, but omitting the side chains and the terminal  $\text{CH}_2\text{OH}$  groups of the ethanolamine tails, the conformation of which was not ascertained. In the later studies, we optimized the conformation of the  $\text{NHCH}_2\text{CH}_2\text{OH}$  tail with respect to the empty gramicidin A backbone [2] and the energy profiles for  $\text{Na}^+$ ,  $\text{K}^+$ ,  $\text{Cs}^+$  were computed [3] introducing explicitly the tail, first frozen in its most stable intrinsic conforma-

tion, then allowed to reoptimize its conformation in the presence of the ion at each step of the progression of the later inside the channel. Recently the possible effect of the amino acid side chains on the energy profiles for  $\text{Na}^+$  was investigated [4] taking into account the role and the flexibility of the ethanolamine end. These studies brought into evidence, in particular, the importance of including all the atoms of the channel, the role of the flexibility of the tail on the energy profiles and the significant contribution of the different tryptophan residues.

In this paper, we present an extension of our computations to the divalent cation  $\text{Ca}^{2+}$ . It is known that gramicidin A is not permeable to  $\text{Ca}^{2+}$  [7,8] which furthermore, when added to the aqueous solution, reduces the conductance of gramicidin A for alkali ions [7–10]. In view of obtaining theoretical informations on the reasons of these

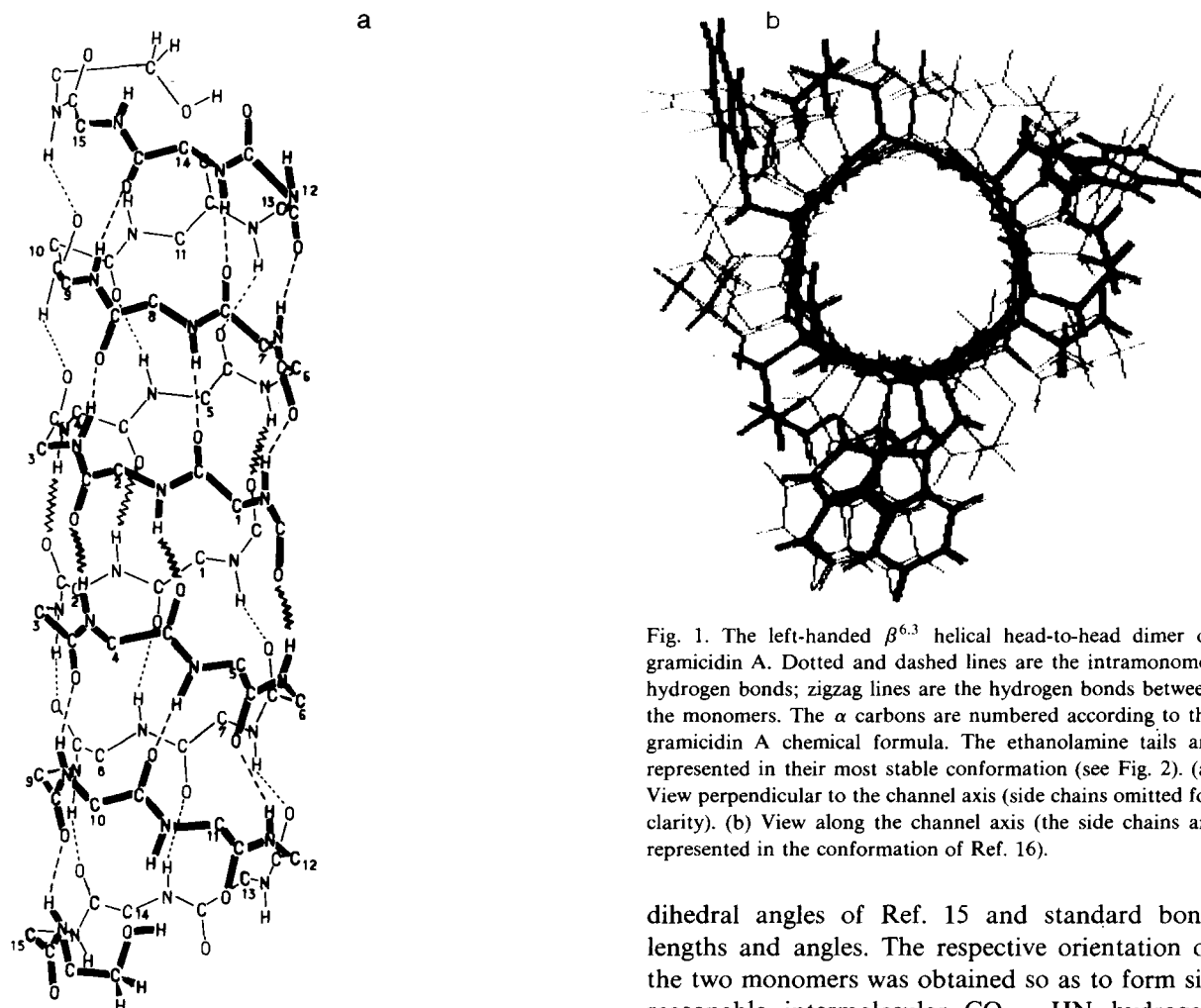


Fig. 1. The left-handed  $\beta^{6.3}$  helical head-to-head dimer of gramicidin A. Dotted and dashed lines are the intramonomer hydrogen bonds; zigzag lines are the hydrogen bonds between the monomers. The  $\alpha$  carbons are numbered according to the gramicidin A chemical formula. The ethanolamine tails are represented in their most stable conformation (see Fig. 2). (a) View perpendicular to the channel axis (side chains omitted for clarity). (b) View along the channel axis (the side chains are represented in the conformation of Ref. 16).

behaviours, we have computed the energy profile for the interaction of  $\text{Ca}^{2+}$  with gramicidin A, investigating in succession the role of the different structural components, polypeptide backbone, ethanolamine tail and amino acid side chains.

### Methodology

The method used for the calculations and summarized in Refs. 1 and 2 is described in detail [11–14]. The inter- and intramolecular energies are calculated as a sum of terms, electrostatic ( $E_{\text{MTP}}$ ), polarization ( $E_{\text{pol}}$ ), repulsion ( $E_{\text{rep}}$ ) dispersion ( $E_{\text{disp}}$ ) and torsional ( $E_{\text{tor}}$ ). The geometry adopted, as in Refs. 1–4 is that of a head-to-head dimer, each monomer being constructed with the  $\phi$ ,  $\psi$

dihedral angles of Ref. 15 and standard bond lengths and angles. The respective orientation of the two monomers was obtained so as to form six reasonable intermolecular  $\text{CO} \cdots \text{HN}$  hydrogen bonds, minimizing geometrically the repulsions of the formyl hydrogens. For the conformations of the amino acid side chains we have adopted, as in Ref. 4, those determined recently as the most stable ones by Venkatachalam and Urry [16]. In order to evaluate the influence of each structural component, three sets of calculations were done: (i) representing gramicidin A by the polypeptide backbone only; (ii) adding to each monomer the ethanolamine tail, fixed first in its intrinsically most stable conformation determined previously [2], then allowed to adopt its preferred conformation with respect to the ion and to the gramicidin A backbone; (iii) including the amino acid side chains with the tail first fixed then flexible. The conformation of the tail is defined [2] by the three dihedral angles given in Fig. 3. For all calcula-

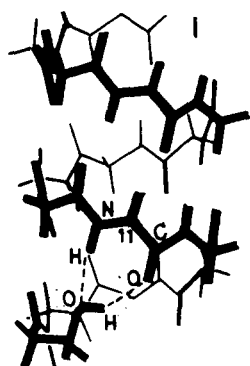


Fig. 2. The most stable conformation of the ethanolamine tail with respect to the rest of the dimer (including or not including the side chains).

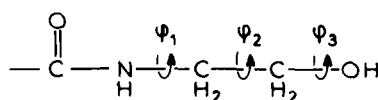


Fig. 3. Torsion angles defining the conformation of the ethanolamine tail.

tions, the conformation of the polypeptide backbone and of the amino acid side chains was maintained rigid. It must be stressed that the most stable conformation of the tail with respect to the backbone in the presence of the side chains was redetermined [4] and found to be the same as in the absence of the side chains [2], namely characterized by the formation of two hydrogen bonds between the end hydroxyl group and the NH and CO group of Trp-11 (Fig. 2). No direct interaction of the tail with the side chains was detected (this being valid provided, of course, that the side chains are in the conformations of Ref. 16). The cation was introduced in successive planes perpendicular to the channel axis, and generally, regularly spaced by 1 Å except in sensitive regions where steps of 0.5 Å were used. In each plane, the cation was allowed to adopt its energy-optimized position.

## Results and Discussion

### (A) Energy profile for $\text{Ca}^{2+}$ , gramicidin A without tail and without side chains

In this study, the  $\text{CH}_2\text{OH}$  group of the ethanolamine end is omitted and replaced by an H atom. The variation of the backbone- $\text{Ca}^{2+}$  interac-

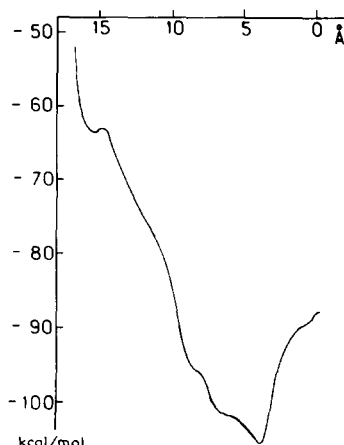


Fig. 4. Energy profile (kcal/mol) for single occupancy by  $\text{Ca}^{2+}$ , gramicidin A without side chains and without ethanolamine tail. Distances in Å from the center of the channel (only half of the profile is given).

tion energy during the hypothetical progression of the cation is represented in Fig. 4. This curve presents a nearly regular descent (with only small local maxima and minima due to the interaction of the cation with different carbonyl oxygens of the L residues) toward a deep minimum ( $-104.8$  kcal/mol) located at 4 Å from the center of the channel. This location is the same as that found for  $\text{Na}^+$  in the same conditions (backbone only [1]) and, apart from a stronger interaction energy for  $\text{Ca}^{2+}$  (due to its double charge) the interactive behaviors of the two ions with gramicidin A are altogether parallel in the same circumstances, involving the presence of a local minimum at the entrance of the channel, a deeper one around 4 Å and a central barrier. Thus, should the channel be made of the backbone only, the  $\text{Ca}^{2+}$  ion, if entering, could follow an easy path down to the minimum at 4 Å, after which it would have to cross a central barrier 17 kcal/mol higher than the local minimum at 4 Å, about twice as much as the barrier found for  $\text{Na}^+$ .

### (B) Energy profile for $\text{Ca}^{2+}$ in gramicidin A with tail but no side chains

#### (1) Tail fixed

When the tail is introduced in its intrinsically preferred conformation, defined by  $\phi_1 = 80^\circ$ ,  $\phi_2 = 65^\circ$ ,  $\phi_3 = 200^\circ$  [2,4], the computed energy profile (curve A of Fig. 5) is significantly different from

that obtained without the tail. The largest differences appear at the entrance of the channel between 16 Å and 13 Å where an appreciable local maximum is observed at 14.5 Å after a first narrow minimum. In all this region the interaction energy is less favorable than in the absence of the tail. This is due to the repulsive contribution of a hydrogen of one of the CH<sub>2</sub> groups of the tail oriented towards the inside of the channel as can be seen in Fig. 1b. From 12 Å inwards, the situation is reversed. This is due to a favorable interaction of Ca<sup>2+</sup> with the oxygen of the hydroxyl group, leading to a deepening of the interaction energy until 5 Å from the center, with local minima at 10.5 Å of -97 kcal/mol and at 6 Å of -107.5 kcal/mol. From 5 Å onwards, the curve A is parallel to the curve of Fig. 4, with the same minimum minimum of -108.4 kcal/mol at 4 Å, the small differences being due to the presence of the oxygen of the hydroxyl group still providing a small attractive contribution in this region. Note that the minimum at 10.5 Å is still higher in energy than the one observed at 4 Å. On the whole for Ca<sup>2+</sup>, the presence of the frozen tail leads to the appearance of a local barrier at 15.4 Å and of local minima at 10.5 and 6 Å from the center, the central barrier being unchanged. Similar features

were observed for Na<sup>+</sup>, upon inclusion of the frozen tail but the two minima at 10.5 and 4 Å were roughly equivalent in energy [3].

## (2) Tail mobile

When the tail is allowed to adopt its optimal conformation with respect to the gramicidin A backbone and to the cation upon the progression of the latter, the energy profile (obtained in the same way as in Ref. 2, namely by subtracting from the total energy computed at each point, the energy of the tail in its intrinsic preferred conformation so as to take into account the variations in energy due to the changes of the conformation of the tail) is represented by curve B in Fig. 5. It is seen that the profile is considerably modified by allowing the flexibility of the tail, essentially in a zone extending from 16 to 9 Å (zone I) characterized by a strong deepening of the energies. The local minimum at 10.5 Å observed in curve A is now the minimum minimum and its value is -117.9 kcal/mol. Note that the local repulsion observed at 14.5 Å has disappeared and is replaced by a small local minimum followed by a very small local barrier at 13.5 Å from the center of the channel. Throughout this region, the calcium ion benefits not only from the attractive interactions with the carbonyl oxygens of the L residues but also from an attractive interaction with the hydroxyl oxygen of the tail, whose conformation is modified so as to optimize the interaction. From 7 Å to the center (zone II), the tail, unable to follow the cation anymore, has recovered its intrinsically preferred conformation and curves A and B are superposed. A high local barrier of about 14 kcal/mol separates the two zones. Between 9 and 7 Å, the tail interacts weakly with the cation, and from 7 Å onwards only a small effect remains. Examination of the evolutions of the  $\phi$ , angles and of the variations of the interatomic distances along the progression shows, similarly to what was observed in Ref. 3, that the two hydrogen bonds stabilizing the intrinsically preferred conformation of the tail (Fig. 2) are broken when the cation is at the exterior of the channel (16 Å) but are progressively reformed during the penetration of the cation inside the channel. These features are all very similar to those observed for Na<sup>+</sup> in the same circumstances, the main difference being that the minimum at 10.5 Å, emphasized by the flexibility

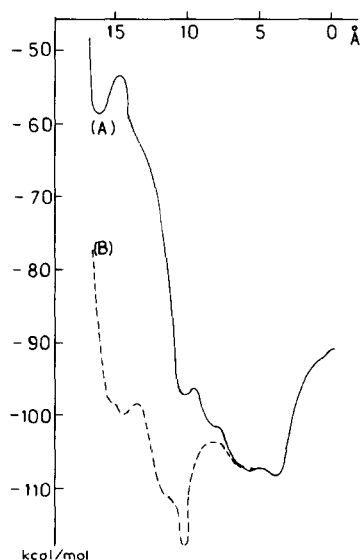


Fig. 5. Same as in Fig. 4 with the ethanolamine tail (A) fixed (full line), (B) mobile (dotted line), but no side chains present.

of the tail, is deeper and narrower for  $\text{Ca}^{2+}$  than for  $\text{Na}^+$ , whereas the local minimum at the mouth of the channel (14.5 Å) is less pronounced for  $\text{Ca}^{2+}$  than for  $\text{Na}^+$ . Nevertheless the flexibility of the tail has approximately the same effect for  $\text{Ca}^{2+}$  as for  $\text{Na}^+$  but differs from the case of  $\text{Cs}^+$  [3].

(C) Energy profile for  $\text{Ca}^{2+}$ , gramicidin A with tail and side chains

The contribution of the amino acid side chains is now analyzed in the same two ways.

(1) Tail fixed

The energy profile for  $\text{Ca}^{2+}$  in the presence of the tail and the side chains is given in Fig. 6, curve A. The comparison of this curve with the corresponding curve A of Fig. 5 indicates that the global effect of the side chains consists of an important increase of the negative interaction energy. The local barrier at 14.5 Å observed in curve A of Fig. 5 has nearly disappeared. Consideration of the equilibrium distances shows that in the early region the cation is considerably displaced out of the channel axis and its position differs from that

observed in the absence of the side chains. It interacts strongly with the carbonyl oxygen of L-Trp-13. Moreover, the minimum of  $-124.30$  kcal/mol observed previously at 6 Å is now the deepest one. But, apart from these two features, the curves A of Figs. 5 and 6 are qualitatively similar.

(2) Tail mobile

The corresponding energy profile obtained when the tail is mobile is given in Fig. 6, curve B. Again, comparing it with curve B of Fig. 5 shows that the effect of the side chains consists essentially of a deepening of the energy. In fact, the curves B of Figs. 5 and 6 are approximately parallel and they both present the same two zones, zone I (between 16.5 and 9 Å) and zone II (between 9 Å and the channel center, where the tail has recovered its intrinsically preferred conformation). In zone I, the small local barrier at 13.5 Å observed in Fig. 5 has now disappeared. Apart from the inversion in the energy order of the two local minima at 6 and 4 Å in zone II, no strong qualitative effects are associated with the presence of the side chains and the barrier separating the two zones remains simi-

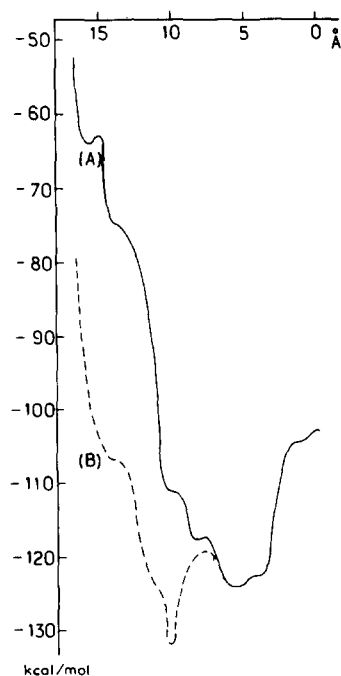


Fig. 6. Same as in Fig. 5 with the side chains and the tail (A) fixed (full line), (B) mobile (dotted line).

TABLE I

EVOLUTION OF THE DIHEDRAL ANGLES  $\phi$  (DEGREES) OF Fig. 3 UPON PROGRESSION OF  $\text{Ca}^{2+}$  IN THE CHANNEL

Z is the distance to the channel center. a, without side chains; b, with side chains.

Z(Å)	$\phi_1$		$\phi_2$		$\phi_3$	
	a	b	a	b	a	b
16.5	38.2	37.5	254.5	256.2	284.4	285.1
16	48.4	50.6	252.9	253.4	280.3	281.5
15.5	83.8	82.6	295.0	296.8	146.9	149.6
15	93.03	93.0	300.9	301.1	147.5	148.3
14.5	105.2	105.1	298.9	298.9	155.7	155.8
14	114.9	115.3	298.3	297.9	163.2	166.5
13.5	124.7	125.3	297.0	295.9	175.5	177.3
13	133.9	133.9	289.5	289.6	189.5	188.8
12.5	139.6	139.1	284.8	288.7	198.5	194.3
12	143.3	142.9	284.8	284.8	214.4	215.1
11.5	147.5	142.7	286.5	286.7	218.2	221.3
11	142.5	141.1	289.0	289.8	236.6	236.3
10.5	131.9	132.3	307.6	307.3	243.2	243.3
10	130.6	129.6	310.03	311.5	258.35	256.0
9	77.2	77.7	49.7	52.8	172.4	169.7
8	78.3	78.2	51.7	51.9	176.2	182.8

TABLE II

DISTANCES (Å) BETWEEN THE CATION AND THE NEAREST CARBONYL OXYGEN FOR TAIL MOBILE IN ZONE I

Z is the distance to the channel center. a, without side chains. b, with side chains

Z(Å)	Carbon to oxygen distance (Å)			
	a		b	
16.5	2.7	Trp-15	2.7	Trp-15
16	2.3	Trp-15	2.3	Trp-15
15.5	2.2	Trp-15	2.2	Trp-15
15	2.3	Trp-15	2.3	Trp-15
14.5	2.4	Trp-15	2.4	Trp-15
14	2.5	Trp-15	2.5	Trp-15
13.5	2.6	Trp-15	2.7	Trp-15
13	3.0	Trp-15	3.0	Trp-15
	3.4	Trp-11	3.3	Trp-11
12.5	2.8	Trp-11	2.8	Trp-11
12	2.6	Trp-11	2.5	Trp-11
11.5	2.6	Trp-11	2.5	Trp-11
11	2.7	Trp-11	2.6	Trp-11
10.5	2.5	Trp-9	2.5	Trp-9
10	2.8	Trp-11	2.9	Trp-11
	2.6	Trp-9	2.6	Trp-9

lar. This similarity can be understood by considering the data collected in Table I which indicates the dihedral angles defining the successive optimal conformations of the tail along the hypothetical progression of the cation: (a) without side chains and (b) with them. These data show clearly that the presence of the side chains has no important effect on the evolution of the conformation of the tail during the progression of the ion. The same results was observed for  $\text{Na}^+$  [4]. Conversely, the presence of the amino acid side chains does not appreciably modify the preferred path of the ion in the channel, as indicated by the successive optimal distances between the cation and the nearest carbonyl oxygen reported in Table II: (a) without side chains, (b) with them. Only worth noting is the closest approach to Trp-11 in the region of the deep minimum. On the whole the energy profile is globally smoothed out and deepened by the inclusion of the amino acid side chains and the calcium ion, if entered, could follow an easy path to the very deep and narrow energy minimum of  $-132 \text{ kcal/mol}$ , after which it would need to jump over two high walls to pass the

center. Inspection of the energy components indicates that the energy lowering contribution of the side chains resides essentially in the polarization terms. This effect was also observed for  $\text{Na}^+$ , although less intense (due to the single instead of double charge). As concerns the central barrier, owing to the deepening of the energy minimum in zone II and the smaller contribution of the side chains at the center of the channel, it manifests an increase to about  $21 \text{ kcal/mol}$ .

In order to analyze in more detail the quantitative effect of the side chains we have reported in Fig. 7 the energy differences between the profiles with and without side chains, for the fixed tail (curve A) and for the mobile tail (curve B). The minima of these curves, which correspond to the largest stabilizing effect of the side chains, occur at  $14.5$ ,  $9$  and  $6 \text{ Å}$  in curve A and at  $9$  and  $6 \text{ Å}$  only in curve B. A similar effect observed for  $\text{Na}^+$  was analyzed (for the tail fixed only) in terms of the individual contribution of the four tryptophan residues  $15$ ,  $13$ ,  $11$  and  $9$ , the sole polar side chains of gramicidin A. The disappearance of the deep minimum in curve B for  $\text{Ca}^{2+}$  incited us to investigate the role of these residues at this point in the profile. This was done by recomputing the profile  $E'$  excluding one tryptophan at a time and considering the difference:  $\Delta = E - E'$  with respect to the corresponding energy  $E$  including all the side chains. The values of  $E'$  and  $\Delta$  are reported in Table III for cases A and B. It is seen that Trp-15 and -9 give a positive contribution while Trp-11 and -13 give a negative one to  $\Delta$ , a feature which can be related to the different orien-

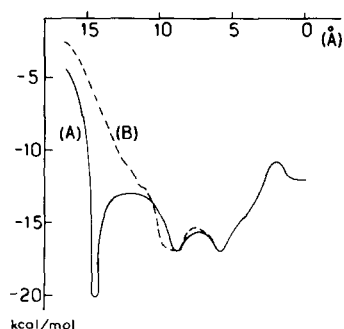


Fig. 7. Energy differences between curves A of Figs. 5 and 6 (A) (full line) and curves B of the same figures (B) (dotted line).

TABLE III

INTERACTION ENERGY  $E'$  OF GRAMICIDIN A WITH  $\text{Ca}^{2+}$  STRIPPED OF ONE TRYPTOPHAN SIDE CHAIN AT A TIME AT 14.5 Å AND CORRESPONDING CONTRIBUTION  $\Delta$  OF EACH TRYPTOPHAN TO THE TOTAL PROFILE WITH ALL SIDE CHAINS (kcal/mol)

	Tail fixed				Tail mobile			
	Trp-15	Trp-13	Trp-11	Trp-9	Trp-15	Trp-13	Trp-11	Trp-9
$E'$	-74.7	-57.7	-71.2	-74.1	-106.8	-103.0	-102.6	-107.8
$\Delta$	1.1	-15.9	-2.4	0.4	0.6	-3.2	-3.6	1.6

tations of the dipole moment of the indole ring in the respective conformations [4]. When the tail is rigid, the contribution of Trp-13 reaches -15.2 kcal/mol, representing 75% of the global contribution of the side chains. When the tail is mobile, the same division of the tryptophans in two groups is observed but the negative contribution of Trp-13 is only -3 kcal/mol, of the same order as that of Trp-11. This is due to the fact that when the tail is mobile it adopts a conformation which constrains the displacements of the cation and limits its approach to the nearest L carbonyl oxygen. Specifically, at 14.5 Å the tail prevents the cation from interacting closely with the L-Trp-13 carbonyl oxygen as it may when the tail is fixed, and a close interaction occurs only with the L-Trp-15 (see Table II). (This does not, of course, prevent the global energy balance to be more favorable than with the tail fixed).

### Concluding remarks

Having described and discussed in some detail the successive results, it seems appropriate to stress the following points:

(a) One clear outcome of this set of calculations is the influence of the different structural components of gramicidin A on the hypothetical energy profile for single occupancy of the channel by the divalent ion  $\text{Ca}^{2+}$ . It is seen that the inclusion of the tail and of its flexibility on the one hand and that of the side chains on the other, modify considerably the energy profile obtained without these contributions, qualitatively as well as quantitatively. The influences of the structural elements on the energy profile for calcium are very reminiscent of the corresponding features observed for sodium

especially as concerns the location of the 'binding site', the overall influence of the amino acid side chains and the role played by the tryptophans as well as its underlying reasons [4]. It is clear that changes in the conformation of the side chains or their substitution could appreciably modify the profile obtained, particularly at the 'entrance' of the channel. A general dramatization of the effects for calcium compared to sodium is observed, due to the much larger coulomb and polarization effects involved here. This dramatization is seen in particular in the values of the energies implied, in the depth and narrowness of the minimum at 10.5 Å and the rapid descent towards it, as well as in the height of the central barrier. Aside from the particular features characteristic of  $\text{Ca}^{2+}$ , we believe that an inescapable conclusion of this step-by-step study is the important effect of each element of the channel in determining the energy profile it generates for an ion.

(b) Concerning the behavior of calcium proper, it is, of course, the profile obtained with the total structure, backbone, side chains, tail mobile, which must be confronted with the known properties. For doing so, it must be recalled that the interaction profiles are all calculated for a bare cation, thus without taking into account the energy necessary to dehydrate it (even partially) at the entrance of the channel. In order to obtain an idea of the 'entrance barrier' due to the dehydration, one can subtract (see Refs. 17, 3 and 5) from our computed energies, the experimental solvation enthalpy which, for  $\text{Ca}^{2+}$ , amounts to -399 kcal/mol [18]. Using the energies computed between 16 and 13 Å from the center (which are between -70 and -110 kcal/mol), the energy balance obtained of over 300 kcal/mol is strongly indicative of an

important barrier at the entrance of the channel, much larger than that computed for the alkali ions in the same fashion [3] (roughly 6-times that for  $\text{Cs}^+$  and 4-times that for  $\text{Na}^+$ ). In spite of the fact that the desolvation of ions at the entrance occurs progressively (unpublished data), and not completely, due to the presence of water in the channel [19–21], the above comparison done under the same conditions is likely to be significant and provides a simple explanation of the apparent difficulty encountered by calcium for penetrating the channel.

Two other features of the present calculations relevant to the lack of permeability of gramicidin A to  $\text{Ca}^{2+}$  are the depth and narrowness of the minimum seen at 10.5 Å and the height of the barriers following it: should the ion overcome the difficulty of entering gramicidin A, it would clearly fall very easily into a site of tight-binding, situated relatively close to the mouth. Striking is the fact that the location of this site is similar to that found for  $\text{Na}^+$ , in agreement with the findings of Urry et al. [22,23] that “a divalent ion can enter the ion binding site” (see also Ref. 8), although it may be remarked that the position inferred from the NMR data for  $\text{Ca}^{2+}$  (and also  $\text{Ba}^{2+}$  [24]) is slightly displaced with respect to that for  $\text{Na}^+$ . Recent spectroscopic data [10] also indicate a calcium binding site close to the ethanolamine terminal of gramicidin A. Further, while the ion encounters no barrier (after the entrance) to fall into the deep site, it requires a strong activation energy (30 kcal/mol) to then pass the center of the channel. Even though the necessary total energy is decomposed in two jumps in the profiles, the most central barrier is appreciably higher than that calculated for  $\text{Na}^+$  (20 against 8 kcal/mol), a feature which would, by itself be sufficient to explain the impermeability of gramicidin A to  $\text{Ca}^{2+}$  (see Ref. 22). Our results seem to indicate that both the depth of the site and the ensuing shape of the profile contribute to the impermeability of gramicidin A to calcium.

(c) The problem of the possible ‘external site’ for  $\text{Ca}^{2+}$  as well as the study of the blocking effect of this ion on the conductance for alkali cations will be dealt with separately together with the effect of the explicit introduction of water at the mouth and in the channel (Etchebest, C. and Pullman, A., unpublished data).

## Acknowledgement

This work was supported by the National Foundation for Cancer Research (Bethesda, MD, U.S.A.) to which the authors wish to express their deep thanks.

## References

- 1 Pullman, A. and Etchebest, C. (1983) FEBS Lett. 163, 199–202
- 2 Etchebest, C. and Pullman, A. (1984) FEBS Lett. 170, 191–195
- 3 Etchebest, C., Ranganathan, S. and Pullman, A. (1984) FEBS Lett. 173, 301–306
- 4 Etchebest, C. and Pullman, A. (1985) J. Biomol. Struct. Dyn. 2, 859
- 5 Urry, D.W. (1971) Proc. Natl. Acad. Sci. USA 68, 672–676
- 6 Urry, D.W. (1973) in Conformation of Biological Molecules and Polymers, The Fifth Jerusalem Symposium on Quantum Chemistry and Biochemistry (Bergman, E.D. and Pullman, B., eds.), pp. 723–734, Israel Academic of Sciences, Jerusalem
- 7 Hladky, S.B. and Haydon, D.A. (1972) Biochim. Biophys. Acta 274, 294–312
- 8 Mayers, V.B. and Haydon, D.A. (1972) Biochim. Biophys. Acta 274, 313–322
- 9 Bamberg, E. and Läuger, P. (1977) J. Membrane Biol. 35, 351–375
- 10 Heitz, F. and Gavach, C. (1983) Biophys. Chem. 18, 153–163
- 11 Gresh, N., Etchebest, C., De la Luz Rojas, O. and Pullman, A. (1981) Int. J. Quantum Chem. Quantum Biol. Symp. 8, 109–116
- 12 Gresh, N., Claverie, P. and Pullman, A. (1984) Theoret. Chim. Acta 66, 1–20
- 13 Gresh, N., Pullman, A. and Claverie, P. (1985) Theoret. Chim. Acta 67, 11–32
- 14 Pullman, A. (1986) Methods in Enzymology, Volume on Biomembranes: Protons and Water, Structure and Translocation (Packer, L., ed.), Academic Press, New York
- 15 Urry, D.W., Venkatachalam, C.M., Prasad, K.U., Bradley, R.J., Parenti-Castelli, G. and Lenaz, G. (1981) Int. J. Quantum Chem. Quantum Biol. Symp. 8, 385–399
- 16 Venkatachalam, C.M. and Urry, D.W. (1984) J. Comput. Chem. 5, 64–71
- 17 Eisenman, G. and Horn, R. (1983) J. Membrane Biol. 76, 197–225
- 18 Goldman, S. and Bates, R. (1972) J. Am. Chem. Soc. USA 94, 1476–1484
- 19 Finkelstein, A. and Andersen, O.S. (1981) J. Membrane Biol. 59, 155–171
- 20 Levitt, D.G., Elias, S.R. and Hautman, J.M. (1978) Biochim. Biophys. Acta 512, 436–451
- 21 Mackay, D.H.J., Berens, P.H., Wilson, K.R. and Hagler, A.T. (1984) Biophys. J. 46, 229–248
- 22 Urry, D.W., Trapane, T.L., Walker, J.T. and Prasad, K.U. (1982) J. Biol. Chem. 257, 6659
- 23 Urry, D.W., Walker, J.T. and Trapane, T.L. (1982) J. Membrane Biol. 69, 225–231
- 24 Urry, D.W., Trapane, T.L. and Prasad, K.U. (1982) Int. J. Quant. Chem. Quant. Biol. Symp. 9, 31–40